# Biomineralization of Arsenate to Arsenic Sulfides is Greatly Enhanced at Mildly Acidic Conditions

**Lucia Rodriguez-Freire**[a,#], **Reyes Sierra-Alvarez**[a], **Robert Root**[b], **Jon Chorover**[b], and **James A. Field**[a]

[a]Department of Chemical and Environmental Engineering, The University of Arizona P.O. Box 210011, Tucson, Arizona, USA

[b]Department of Soil, Water and Environmental Science, The University of Arizona P.O. Box 210038, Tucson, Arizona, USA

## Abstract

Arsenic (As) is an important water contaminant due to its high toxicity and widespread occurrence. Arsenic-sulfide minerals (ASM) are formed during microbial reduction of arsenate ($As^V$) and sulfate ($SO_4^{2-}$). The objective of this research is to study the effect of the pH on the removal of As due to the formation of ASM in an iron-poor system. A series of batch experiments was used to study the reduction of $SO_4^{2-}$ and $As^V$ by an anaerobic biofilm mixed culture in a range of pH conditions (6.1–7.2), using ethanol as the electron donor. Total soluble concentrations and speciation of S and As were monitored. Solid phase speciation of arsenic was characterized by x-ray adsorption spectroscopy (XAS). A marked decrease of the total aqueous concentrations of As and S was observed in the inoculated treatments amended with ethanol, but not in the non-inoculated controls, indicating that the As-removal was biologically mediated. The pH dramatically affected the extent and rate of As removal, as well as the stoichiometric composition of the precipitate. The amount of As removed was 2-fold higher and the rate of the As removal was up to 17-fold greater at pH 6.1 than at pH 7.2. Stoichiometric analysis and XAS results confirmed the precipitate was composed of a mixture of orpiment and realgar, and the proportion of orpiment in the sample increased with increasing pH. The results taken as a whole suggest that ASM formation is greatly enhanced at mildly acidic pH conditions.

### Keywords

Arsenate reduction; sulfate reduction; bioprecipitation; orpiment; realgar; biomineralization

[#]Corresponding author: Department of Chemical and Environmental Engineering, University of Arizona, P.O. Box 210011, Tucson, Arizona Tel. 520-621-2591 Fax. 520-621-6048 luciar@email.arizona.edu.

## 1. Introduction

Arsenic (As) contamination of natural waters is a major health and environmental concern. The United States Environmental Protection Agency (US-EPA) have set the As standard in drinking water at 10 ppb (US-EPA 2001). The concentration of As in groundwater and drinking water exceeds this limit in many locations across the world (Murcott 2012). Elevated As concentrations generally occur due to As mobilization from high As-content rocks and sediments driven by changes under the biogeochemical conditions of the aquifer (Welch et al. 2000), therefore a better understanding of the biogeochemistry of As is necessary to predict and control As mobilization and to remediate As contaminated waters.

Arsenopyrite (FeAsS), realgar (AsS) and orpiment ($As_2S_3$) are naturally formed As-bearing sulfide minerals (ASM) (O'Day et al. 2004) which are known to be a source of As contamination due to weathering processes that dissolve the mineral and release the retained As into the environment (Welch et al. 2000). However, the formation of ASM can be harnessed to promote the immobilization of As. The biogeochemical cycle of As is dominated by the microbial transformations between the two main inorganic species of As, arsenate ($As^V$, $H_2AsO_4^-$ and $HASO_4^{2-}$ in circumneutral environments) and arsenite ($As^{III}$, $H_3AsO_3$) (van Lis et al. 2013). In oxidizing environments, $As^V$ is the predominant species, and the accumulation of As is limited by sorption processes of As on iron (Fe) oxides and oxyhydroxides surfaces (Jonsson and Sherman 2008); in reducing environments, $As^V$ can be microbially reduced to $As^{III}$ (van Lis et al. 2013). While $As^{III}$ is also adsorbed onto Fe oxides and oxyhydroxides, it's sorption strength with Fe surface complexation is weaker than $As^V$ (Jonsson and Sherman 2008). In environments where Fe is lacking and sulfur (S) is present, the solubility of As is potentially controlled by the precipitation of As in ASM (O'Day et al., 2004). The predominant species of S are sulfide ($H_2S$) and sulfate ($SO_4^{2-}$), the most reduced and oxidized species, respectively. Microorganisms oxidize or reduce S depending on the redox conditions present in the aquifer (Tang et al. 2009). The microbial reduction of $As^V$ and $SO_4^{2-}$ can cause the biomineralization of As and ASM will be formed (Newman et al. 1997).

Recent evidence demonstrates the biological nature of the formation of ASM. Rittle (1995) first proved the precipitation of $As^{III}$ was due to biological $SO_4^{2-}$ reduction. In 1997, Newman (1997) discovered a new bacterial strain *Desulfotomaculum auripigmentum* sp. OREX-4 which was able to precipitate $As_2S_3$ through the heterotrophic reduction of $As^V$ and $SO_4^{2-}$. The biological precipitation of AsS by a thermophilic bacterium *Caloramator* strain YeAs (Ledbetter et al. 2007) and by a hyperthermophilic archaea *Pyrobaculum arsenaticum* sp. PZ6 (Huber et al. 2000); and, the formation of AsS nanotubes by *Shewanella* strains (Lee et al. 2007) have reinforced the evidence of ASM biogenesis. Furthermore, Demergasso (2007) has demonstrated the biological origin of $As_2S_3$ in Andean sediments by analyzing the sulfur isotope ratios ($^{34}S/^{32}S$) in chemically and biologically formed ASM, and comparing it with the minerals found in the sediments. In addition, Saunders (2008) evaluated the effect of $SO_4^{2-}$ and electron donor addition on the As mobility in As contaminated groundwater, which resulted in a decrease of the dissolved As in the aquifer, attributed to the formation of FeAsS.

Several lab-scale experiments, conducted in microcosm or bioreactors, have been performed to study the biological precipitation of ASM at circumneutral or acidic pH. Most of these experiments studied the precipitation of ASM in Fe-containing systems (Kirk et al. 2010, Onstott et al. 2011). Fe-sulfide minerals, such as pyrite ($FeS_2$) or mackinawite (FeS) have lower solubility than the ASM, therefore they would precipitate first removing Fe and S from solution (Kirk et al. 2010, O'Day et al. 2004). In high $SO_4^{2-}$ waters, Fe would become limited and the system would essentially behave as an Fe-poor environment, stressing the importance of understanding the formation of ASM in the absence of Fe.

The objective of this study was to determine the effect of the pH on the rate, extent and type of biological ASM formation in Fe-poor environments. In order to attain this objective, a series of batch experiments, with pH conditions ranging from 6.1 to 7.2, were performed using an anaerobic biofilm mixed culture as inocula with only trace levels of Fe. The batch experiments were amended with $As^V$ and $SO_4^{2-}$, and ethanol was used as electron donor. The main reactions occurring in the microcosms are summarized in Table 1. The precipitation of ASM was evaluated by measuring the total As and S concentration and speciation in solution. Likewise the solid phase was characterized by different spectroscopic techniques.

## 2. Materials and Methods

### 2.1. Source of microorganisms

An anaerobic granular biofilm was obtained from full scale upflow anaerobic sludge bioreactor (UASB) from a beer brewery wastewater treatment plant Mahou (Guadalajara, Spain) (0.042±0.002 g volatile suspended solids (VSS)/g wet wt). The sludge was examined for As content, and As level was below detectable limits (digestion of sludge using aqua regia and further analysis in the ICP-OES, see section 2.6. Analytical methods).

### 2.2. Medium composition

The basal medium was prepared using ultra pure water (Milli-Q system; Millipore) and contained (mg/L): $K_2HPO_4$ (600); $NaH_2PO_4.2H_2O$ (899); $NH_4Cl$ (280); $MgCl_2{\cdot}6H_2O$ (83); $CaCl_2.2H_2O$ (10); yeast extract (20), and 1 mL/L of a trace element solution that was added to the medium to provide a final concentration of (μg/L): $FeC1_3{\cdot}4H_2O$ (2,000); $CoCl_2{\cdot}6$ $H_2O$ (2,000); $MnCl_2{\cdot}4$ $H_2O$ (500); $AlCl_3{\cdot}6$ $H_2O$ (90); $CuCl_2{\cdot}2H_2O$ (30); $ZnCl_2$ (50); $H_3BO_3$ (50); $(NH_4)_6Mo_7O_{24}{\cdot}4$ $H_2O$ (50); $Na_2SeO_3{\cdot}5$ $H_2O$ (100); $NiCl_2{\cdot}6H_20$ (50); EDTA (1,000); resazurin (200); HCl 36% (1 μL). 0.75 mM of $SO_4^{2-}$ was added as $Na_2SO_4$ and 0.5 mM of $As^V$ $Na_2HAsO_4.7H_2O$. The electron donor used was ethanol to a final concentration of 12 mM by adding 283.3 μL/L. The experiments were flushed with $N_2/CO_2$ (80:20) to ensure anaerobic conditions. $NaHCO_3$ was used to control the pH of the solution from 6.1 (0.4 g/L $NaHCO_3$), 6.5 (1 g/L $NaHCO_3$), 6.85 (2 g/L $NaHCO_3$) and 7.2 (4 g/L $NaHCO_3$). 1.5 g VSS/L of sludge was added to the treatment, after being sieved and clean with Milli-Q water to remove any soluble contaminant.

### 2.3. Experimental incubations

The biomineralization of ASM was evaluated in batch mode in 160 mL serum bottles containing 120 mL of the liquid medium. The liquid phase was flushed with $N_2/CO_2$ (80:20) for 10 min, then the 34 μL of ethanol were added to the proper treatments and quickly sealed with rubber septa and aluminum crimp seal. The headspace was flushed for 5 min. needle in-needle out with $N_2/CO_2$ (80:20). The treatments were run in triplicate with one bottle dedicated to pH measurements and solid phase analysis. Proper controls were set up in parallel to ensure the fidelity of the results. These controls were: (i) non-inoculated with $As^V$ and ethanol, $SO_4^{2-}$ and ethanol, or both, $As^V$ and $SO_4^{2-}$, and ethanol; (ii) inocula with just one of the electron acceptors and the ethanol; (iii) inocula with no electron acceptor; and, (iv) inocula with one electron acceptor but no ethanol. Non-inoculated controls were prepared under sterile conditions and the medium was autoclaved at 121°C for 10 min. In the non-inoculated controls, ethanol was added after autoclaving to avoid degradation. The assays were incubated at 30°C in the dark, and in an elliptical shaker (115 rpm).

### 2.4. Pourbaix diagrams

Pourbaix diagrams ($E_h$-pH diagrams) were used to understand the formation and stability of ASM for the experimental conditions (0.5 mM $As^V$, 0.25 mM $SO_4^{2-}$) The thermodynamic data was obtained from Visual MinTEQA2 and National Bureau of Standards (NBS) databases and the diagrams were built using the W32-Stabcal modeling software.

### 2.5. As removal rate calculation

The As removal rate was obtained by calculating the slope for the percentage of As removal over time during the experiment, defined by the following equation:

$$\%\text{As Removal Rate} = \left[\frac{\Delta\,(\%\text{As Removal})}{\Delta\,(\text{t})}\right]_0^{\text{t}} \quad \text{Eq. 7}$$

The As removal rate was calculated for the period of increasing As removal until the steady state was reached.

### 2.6. Analytical methods

Liquid samples were taken from sealed serum flasks by piercing the stoppers using sterile syringes with 16-gauge needles. All samples were centrifuged (10 min, 14,000 g) after sampling and stored in polypropylene vials. $As^V$ and $SO_4^{2-}$ were analyzed by suppressed conductivity ion chromatography using a Dionex IC-3000 system (Sunnyvale, CA, USA) fitted with a Dionex IonPac AS11 analytical column (4 × 250 mm) and AG16 guard column (4 mm × 40 mm). The injection eluent (KOH) was 30 mM for 10 min. Total As concentration was measured by using an inductively coupled plasma-optical emission spectrometry (ICP-OES) system model Optima 2100 DV from Perkin–Elmer TM (Shelton, CT, USA) monitored at wavelength 193.7 nm. $H_2S$ was determined using the methylene blue method described by Truper (1964) and measured using an UV-visible spectrophotometer (Agilent 8453, Palo Alto, CA, USA). The measurement of $H_2S$ provides the amount as $H_2S$ in the liquid phase only. The total concentration of $H_2S$ was calculated by considering the speciation of $H_2S$ at the measured pH using the dissociation constants

and the partition of $H_2S$ between the liquid medium and the headspace at the incubation temperature.

Headspace samples in the batch experiments were taken with a pressure lock gas tight syringe (1710RN, 100 µl (22s/2″/2), Hamilton Company). Ethanol, acetate and $CH_4$ were monitored in an Agilent Technologies 7890A gas chromatography system with a Restek Stabilwax®-DA Column (30 m × 0.35 mm, ID 0.25 um) with flame ionization detector, and He used as a carried gas.

Solid samples were taken under anaerobic conditions inside the anaerobic chamber (COY Laboratory Products Inc., Grass Lake, MI), to avoid any oxidation of the mineral. The solid samples were obtained by homogenizing and concentrating by centrifugation the solid phase contained in 50 mL to 1.5 mL. The solid phase was cleaned by centrifuging and replacing the supernatant with $O_2$ free Milli-Q water obtained by adding 100 mL of Milli-Q water to a 160 mL serum bottle, and flushing it following the same procedure than for the experimental incubations. Solid phase was characterized using a Scanning Electron Microscopy (SEM) combined with energy dispersive spectroscopy (EDS), and K-edge X-ray absorption spectra (XAS) with X-ray absorption near-edge structure (XANES) and extended x-ray absorption fine-structure (EXAFS) according to the methodology previously described in the Supplementary Information (SI).. Measurements of pH, $E_h$ and VSS were conducted according to standard methods (APHA 1999).

## 3. Results

### 3.1. As and S biological transformations

The biological transformation of As and S and the precipitation of ASM was evaluated at three different pH conditions (6.1, 6.5 and 7.2) using ethanol as electron donor. Fig. 1 shows the evolution of $As^V$ (A), total As (B), $SO_4^{2-}$ (C) and total $H_2S$ (soluble + volatile) (D), over the incubation time of the experiment at pH 6.1. Both $As^V$ and $SO_4^{2-}$ reduction were required for the formation of ASM to occur. When $SO_4^{2-}$ was not amended in the treatment, $As^V$ became reduced but the total As concentration in solution was not affected. Similarly, when $As^V$ was not added to the treatment, $SO_4^{2-}$ concentration decreased with a stoichiometric increment in $H_2S$ concentration. But, when $As^V$ and $SO_4^{2-}$ were incubated together, the total As and S concentrations decreased, and 100% of the total As was removed in only 9 d. Therefore, both the reduction of $As^V$ and $SO_4^{2-}$ must occur for the formation of ASM, as evidenced by the loss of total aqueous As and S.

The importance of the electron donor was evaluated in controls lacking ethanol. The addition of the electron donor was essential for ASM formation by promoting the reduction of $SO_4^2$, which was limited in the controls lacking ethanol. Compared to the full treatment, the rate of $SO_4^{2-}$ reduction in the absence of ethanol was 4.1-fold lower during the critical time period (days 1 and 9) when arsenic was being removed in the full treatment. In contrast, the rate of $As^V$ reduction in the treatments without ethanol was as fast as in the ethanol-amended treatments. The addition of the electron donor greatly boosted the $SO_4^{2-}$ reduction rate, enabling the formation of ASM.

The reduction of $As^V$ and $SO_4^{2-}$ in the non-inoculated controls was not noteworthy in comparison with the inoculated treatments. Total As and total S decreased by 10.7±2.6% and 21.6±2.9% respectively in non-inoculated treatments including both $As^V$ and $SO_4^{2-}$. What little removal that did occur took place at the start and thereafter the concentrations were stable. The lack of important changes in the non-inoculated controls indicates that abiotic reactions are relatively unimportant compared with the biological reactions, stressing the significance of the biological transformations of As and S under the studied conditions.

The amount of total As and S removed in the treatments can be calculated by applying a mass balance in the system. The ratio of S loss to As loss ($S_{loss}/As_{loss}$) was used to predict mineral phase precipitation based on the expectation that an S/As of 1.5 and 1.0 corresponds to $As_2S_3$ and AsS, respectively. Fig. 2 compares the mass balances for S and As between different inoculated treatments after 35 d incubation at pH 6.1. In the absence of $As^V$, all the $SO_4^{2-}$ reduced was recovered as $H_2S$, but if $As^V$ was amended to the treatment, 0.71 mM of S as $H_2S$ was missing from the experiment. Similarly, the total As concentration hardly decreased (15.3% of the total As) without $SO_4^{2-}$ but the decrease was substantial (100% of the total As) if $SO_4^{2-}$ was present in the treatment. The resulting $S_{loss}/As_{loss}$ ratio corresponded to 1.29 in the treatment amended with $As^V$ and $SO_4^{2-}$. These results suggest the formation of a mixture of AsS and $As_2S_3$.

The formation of ASM was confirmed by visual observation of a yellow precipitate just in the inoculated assays containing $SO_4^{2-}$ and $As^V$. The formation of the mineral could be appreciated with the naked eye after 5 d of incubation. The amount of precipitate increased and the difference in the color of the medium between the complete inoculated treatment and the control missing $As^V$ was very intense at day 12 (Fig. S1).

### 3.2. Role of pH on the precipitation of ASM and the removal of As

Two additional experiments were performed at pH 6.5 and 7.2. Similar as the results obtained for pH 6.1, As and S removal from solution was only significant in inoculated treatments containing both $As^V$ and $SO_4^{2-}$. However, the extent and rate of As and S removal as well as the $S_{loss}/As_{loss}$ ratios varied depending on the pH. Table 2 provides the total As, $SO_4^{2-}$, $H_2S$, pH and $S_{loss}/As_{loss}$ ratio at five different times over the experiment for the three pH conditions, for the inoculated treatment with $As^V$ and $SO_4^{2-}$ amended with ethanol. The total loss of soluble As and S decreased as the pH conditions of the assay increased, which corresponded to more of the biogenic $H_2S$ from $SO_4^{2-}$ reduction being recovered in the medium (especially at pH 7.2). The ratio $S_{loss}/As_{loss}$ was 1.25 to 1.47 for the treatments at pH 6.1 and 6.5, but higher ratios were observed on days 9 and 12 at pH 7.2 (Table 2). These results suggest a pH dependence of the As removal and ASM formation.

The rate and extent of As removal was greatly impacted by the pH. Fig. 3 compares the percentage of As removal as a function of time for the three pH treatments. The percentage of As removed over the entire experiment was 93.9±0.6% and 77.9±0.8% at pH 6.5 and 7.2, respectively. The relationship between the extent and rate of As removal as a function of the pH is shown in Fig. 4. An inversely proportional dependency between the As removal and As removal rates was observed with pH. The percentage of As removed after 9 days was 2-fold higher at pH 6.1 than at pH 7.2. The rate of As removal was 3.4-fold higher at pH 6.1

than at pH 7.2 over the first 9 d of the experiment, and then it increased to 17-fold higher after $H_2S$ started to accumulate at pH 7.2. The data fit with a linear equation over the pH range with a high correlation (R-squared values higher than 0.94). The results indicate a sharp pH-dependency in the near neutral range, with large rate enhancements at mildly acidic conditions.

An independent set of experiments was performed with an older sample of the anaerobic biofilm at different pHs. The same relationship was observed between As removal extent and rate as a function of the pH (results are shown in the Supplementary Data). The percentage of As removed was higher at the lower pH over a long term incubation. As removal and As removal rate were inversely proportionally dependent on the pH and the data also had a near perfect a linear equation, with a negative slope and a high correlation. The reproducibility of the results with a different sample of the anaerobic biofilm serves to validate the dependency of biogenic ASM formation on pH.

### 3.3. Mineral characterization

Solid samples from the three treatments were analyzed using SEM-EDS. Small particles of ASM were present as aggregates and on the surface of the bacteria. Fig. 5 provides an SEM image and EDS analysis for two different points, on the surface of a bacterium (Point 1) and on a mineral aggregate (Point 2). The micrograph shows different bacteria surrounded by minerals. The EDS analysis demonstrates that the minerals are composed of As and S. These results confirm the close association between bacteria and mineral formation, supporting a microbial role in the formation of ASM. The solid mineral samples were further characterized using XAS.

XAS enabled the identification of As coordinative environment in precipitates formed at the two pH extremes of the conditions evaluated in the experiments (pH 6.1 and 7.2). Fig. 6A shows the XANES spectra for the two analyzed samples along with those of reference AsS and $As_2S_3$. The main XANES peak absorbance for $As_2S_3$ was shifted to slightly higher energy relative to that for AsS. However, this shift was within the resolution at the As edge and should not be used as a sole diagnostic for As coordinated in an $As_2S_3$ versus AsS structure. Fig. 6B shows the EXAFS spectrum of the two analyzed samples and the reference minerals. The solid formed at pH 6.1 had high similarity with AsS, but lacks the deep troughs of the AsS spectra at 7 to 8 and 9 to 10 k($Å^{-1}$), suggesting the additional presence of $As_2S_3$ in the sample. The spectrum of the mineral formed at pH 7.2 is more similar to orpiment, but seemed to fall between the two mineral references. Linear combination fitting (LCF) of As K-edge EXAFS data suggests that the mineral formed at pH 6.1 was a mixture of AsS with $As_2S_3$, while the mineral formed at pH 7.2 corresponds more closely to $As_2S_3$, 63% AsS and 27% $As_2S_3$ and 38% AsS and 66% $As_2S_3$, respectively (sum ≠ 100% because the fits were not normalized).. The XANES fits indicated that the speciation of the pH 6.1 sample was 65% AsS and 33% $As_2S_3$ and the speciation of the pH 7.2 sample was 32% AsS and 67% $As_2S_3$. The occurrence of AsS and $As_2S_3$ was fully confirmed by the XAS characterization.

### 3.4. Ethanol as the electron donor source and the production of acetate and $CH_4$

In order to monitor the electron-donating process, the conversion of ethanol to acetate and $CH_4$ was measured. The degradation pathway of ethanol to $CH_4$ by the microbial consortium in the anaerobic biofilm can be evaluated by studying the treatment lacking $As^V$ and $SO_4^{2-}$ addition. Ethanol is transformed to acetate and hydrogen ($H_2$) by acetogenic bacteria (Eq. 1). Both acetate and $H_2$ are used by methanogens (Eq. 2 and 3) to produce $CH_4$. As can be appreciated in Fig. 7, in the treatment missing $SO_4^{2-}$ and $As^V$, ethanol concentration decreased quickly after just one day of incubation, accompanied by a small initial accumulation of acetate and subsequently the formation of $CH_4$. $CH_4$ production increased rapidly until reaching a concentration of 8.7±0.4 mmol/$L_{liq}$. Thereafter, $CH_4$ kept increasing for the rest of the experiment at a lower rate. By the end of the experiment, the production of $CH_4$ was 13.9±0.7 mmol/$L_{liq}$. These results illustrate the rapid transformation of ethanol to acetate and subsequently to $CH_4$. The addition of $As^V$ and $SO_4^{2-}$ to the treatments can potentially impact the utilization of ethanol since electron equivalents ($e^-$ eq) could be used for their reduction. The $H_2S$ and $As^{III}$ formed from the reduction could potentially inhibit the activity of the methanogens.

Ethanol utilization rate was the same in the presence or absence of $SO_4^{2-}$, indicating that the addition of $SO_4^{2-}$ and its reduction to $H_2S$ did not affect the metabolic activity of acetogens. In addition, the pattern of acetate accumulation and subsequent consumption as well as the profile of $CH_4$ production was similar in both cases. The $CH_4$ production was however slightly lower in the presence of $SO_4^{2-}$. The difference between the $CH_4$ produced was 1.1 mmol/$L_{liq}$, since 3.2 mmol/$L_{liq}$ of $H_2$ would be required to reduce the supplied 0.8 mM of $SO_4^{2-}$ to $H_2S$, 0.8 mmol/$L_{liq}$ less $CH_4$ would have been expected in the treatment with $SO_4^{2-}$. This analysis supports the expectation that $H_2$ from ethanol conversion was utilized as the electron donor for $SO_4^{2-}$ reduction.

The inhibitory impact of $As^V$ to the acetogenic and methanogenic activity was also evaluated. The presence of As greatly reduced the rate of ethanol conversion, and it inhibited the methanogenic activity. Ethanol concentration decreased at a much lower rate in the presence compared to the absence of As. In the presence of As, the acetate concentration increased until day 5, when it reached 5.1±0.9 mM; thereafter, the concentration was stable until the end of the experiment. The accumulated acetate was clearly not being used as a substrate by the methanogens to produce $CH_4$. $CH_4$ formed slowly throughout the course of the experiment, and the production rate was approximately 10-fold less than in the treatment with no As. These results demonstrates that the presence of As can delay the utilization of ethanol by acetogenic bacteria, and it greatly inhibit the acetoclastic methanogenic activity.

In treatments receiving both $SO_4^{2-}$ and $As^V$, the formation of ASM reversed the methanogenic inhibition by As. The inhibition reversal did not occur immediately but instead corresponded to the moment in time when full precipitation of ASM minerals occurred on day 8 (Fig. 7). Consequently during the first 8 days, the full treatment (receiving both $As^V$ and $SO_4^{2-}$) behaved the same as the treatment with just $As^V$ addition. There was a delay in the ethanol utilization, with an initial accumulation of acetate and no $CH_4$ production in both cases (Fig. 7). On day 9, after the entire total soluble As was removed

(Fig. 1) due to ASM precipitation, the inhibition reversed. The accumulated acetate decreased to low levels and the $CH_4$ production all of sudden commenced, reaching a final production of 8.9±0.9 mmol/$L_{liq}$ (Fig. 7). Therefore, the removal of As by the biogenic formation of ASM rendered the As non-bioavailable and thus the As was no longer capable of causing microbial toxicity.

## 4. Discussion

The results taken as a whole demonstrate that the biological reduction of $As^V$ and $SO_4^{2-}$ by an anaerobic mixed culture biofilm leads to the formation of ASM in Fe-poor environments, leading to the immobilization of As to non-bioavailable forms. The biomineralization of the ASM depended strongly on the pH conditions in the near neutral range. The amount and rate of As removal were highly enhanced at mildly acidic conditions. Ethanol was readily used as an electron donor source to stimulate the reduction of $As^V$ and $SO_4^{2-}$. The presence of soluble As was found to completely inhibit the activity of the methanogens in the biofilm inoculum; however, the insolubilization of As by biogenic ASM formation reversed the inhibition.

### 4.1. Microbial reduction of $As^V$ and $SO_4^{2-}$ promotes the bioprecipitation of ASM

The biogenic formation of ASM can be attained by the combined reduction of $As^V$ and $SO_4^{2-}$. A mixed culture biofilm from a methanogenic environment, which was not previously exposed to high As levels, readily reduced $As^V$. $As^V$ and $SO_4^{2-}$ can be biologically reduced by a pure or by a mixed culture. Several $SO_4^{2-}$-reducing bacteria have been reported as $As^V$-reducing bacteria (Macy et al. 2000). But only five strains of three bacterial genera, *Desulfotomaculum* (Newman et al. 1997), *Caloramator* (Ledbetter et al. 2007) and *Shewanella* (Lee et al. 2007) have been reported to precipitate $As_2S_3$, AsS and As-S nanotubes, respectively; and, a hyperthermophilic archaea genus, *Pyrobaculum* (Huber et al. 2000) can precipitate AsS. However, the presence of $As^V$ and $SO_4^{2-}$ -reducers in a mixed culture has been proven to promote the precipitation of ASM in natural environments (Demergasso et al. 2007, Saunders et al. 2008) as well as in a laboratory scale bioreactor (Battaglia-Brunet et al. 2012). In this study, the anaerobic mixed culture biofilm reduced $As^V$ and $SO_4^{2-}$ when both were amended into the same treatment, causing biogenesis of ASM which effectively immobilized the soluble As. The natural co-occurrence between $As^V$ and $SO_4^{2-}$-reducing bacteria can explain the ability of anaerobic microorganisms to promote the bioprecipitation of ASM.

The addition of ethanol as exogenous electron donor was not a requirement to achieve $As^V$ reduction. In the treatments lacking ethanol, there are two sources of $e^-$ eq to support the reduction of $As^V$, the endogenous decay of the mixed culture biofilm and the degradation of the yeast extract amended to support the growth of the biofilm. The potential of methanogenic sludge to reduce $As^V$ without the addition of an electron donor has been reported before (Sierra-Alvarez et al. 2005). Furthermore, the contribution of the endogenous substrate decay in a comparable methanogenic biofilm corresponded to 16–21 $e^-$ meq/g VSS, available due to the hydrolysis of biomass in the sludge over 30 d (Tapia-Rodriguez et al. 2010). The initial rate of endogenous decay was found to be 0.4 to 1.1 $e^-$

meq/g VSS.d. According to these results, the biofilm can donate 24–31 $e^-$ meq/L electron donor at a rate of 0.6–1.7 $e^-$ meq/L.d with the 1.5 gVSS/L used in the experiments. In addition to the $e^-$ eq donated by the endogenous substrate decay, the degradation of the yeast extract (20 mg/L) could provide up to 3.1 $e^-$ meq/L. Therefore, the amount of $e^-$ eq released by the decay of the biofilm and the yeast extract would be more than ample to support the reduction of 0.5 mM of $As^V$ (1 $e^-$ meq/L).

The addition of an exogenous electron donor greatly enhanced $SO_4^{2-}$ reduction. This coincided with a previous study where ethanol was found to be an effective electron donor promoting enhanced $SO_4^{2-}$ reduction in an anaerobic granular sludge biofilm beyond the endogenous rate (Liu et al. 2010). The reduction of 0.8 mM of $SO_4^{2-}$ to $H_2S$ requires 6.4 $e^-$ meq/L, which are available from the endogenous substrate decay and the degradation of yeast extract; however, an initial competition between $SO_4^{2-}$-reducing bacteria and methanogens delayed the reduction of $SO_4^{2-}$. The competition for $e^-$ eq between $SO_4^{2-}$-reducing bacteria and methanogens has been reported in several studies in the past. $SO_4^{2-}$ reducers will outcompete methanogens for the electron donor utilization, since they have a higher substrate affinity for $H_2$, but an initial competition would occur due to lower initial numbers of $SO_4^{2-}$ reducers than methanogens in a methanogenic sludge (Elferink et al. 1994).

### 4.2. Slightly increasing the pH decreased the amount of As removal and percentage of AsS in the mineral

Small variations in the pH affected the removal of As from the system. The extent and rate of As and S removal from aqueous solution were highest at the lower pH conditions corresponding to mildly acidic pH values. When the pH increased, less $H_2S$ was removed due to ASM formation. High $H_2S$ concentrations at neutral pH are known to favor the formation of thioarsenite species (Wilkin et al. 2003), limiting the elimination of soluble As by biomineralization. Newman (1997) studied the chemical precipitation of $As_2S_3$ at different pH values and different $H_2S$ concentrations. $As_2S_3$ was readily precipitated at pH lower than 7 but not at higher pH values when the $H_2S$ concentration was 0.1 mM. Increasing the $H_2S$ concentration to 1 mM caused the minimum pH required for $As_2S_3$ precipitation to decrease to 6.6.

ASM formation is impacted by the stoichiometry of the available $As^{III}$ and $H_2S$, which will be dictated by the reduction of $As^V$ and $SO_4^{2-}$. Microorganisms gain more energy from the dissimilatory reduction of $As^V$ compared to $SO_4^{2-}$ reduction, thus $As^V$ reduction is expected to proceed first. A bioenergetic analysis of the redox pair shows that $As^V/As^{III}$ has higher standard reduction potential (60 mV) than $SO_4^{2-}/H_2S$ (−220 mV) (Hoeft et al. 2004). In this study, $As^V$ was reduced first prior to $SO_4^{2-}$ reduction, but it is not clear if it was due to an energetic advantage or the fact that there was a 2 d lag phase before $SO_4^{2-}$ reduction started, both in the presence and in the absence of $As^V$. Hence, $As^{III}$ was already formed before $H_2S$ started to accumulate, favoring the biomineralization of $As^{III}$-$H_2S$ and removing $H_2S$ from the medium. This conclusion is in agreement with the observations made by Newman (1997). *D. auropigmentum* first reduced $As^V$ and then $SO_4^{2-}$, allowing the precipitation of $As_2S_3$, while another tested bacterium, *Desulfobulbus propionicus*, that quickly reduced

$SO_4^{2-}$ before reducing $As^V$, was not able to promote the formation of ASM. The concomitant reduction of $As^V$ and thiosulfate ($S_2O_3^{2-}$) by *Shawanella* strain HN-41 also promoted the precipitation of As-S nanotubes (Lee et al. 2007). Therefore, biological activity can enhance the precipitation of ASM by controlling the rate of $As^{III}$ and $H_2S$ formation in a favorable stoichiometric ratio.

The pH changes also affected the mineralogy of the precipitate. The $S_{loss}/As_{loss}$ ratio and XAS analysis showed an increase in $As_2S_3$ proportion over AsS at the higher pH values. The stoichiometric calculations from the $S_{loss}/As_{loss}$ ratios indicates 70% AsS and 30% $As_2S_3$ at pH 6.1 which are in good agreement with XAS characterization results of the solid phase. However, the ratios during days 9 and 12 at pH 7.2 indicate 100% $As_2S_3$ which differs from the solid characterization results, 67% and 66% orpiment by XANES and EXAFS respectively. A plausible explanation is that both the stoichiometric ratio and the spectral data obtained for pH 7.2 have a higher associated error compared to data obtained at pH 6.1. Nevertheless, both the solid characterization and the stoichiometric ratio analysis correctly predict an increase in $As_2S_3$ percentage with increasing pH. The relationship between the mineral phase proportion and the pH has not been studied before. The difference in behavior with pH can be explained by thermodynamic relationships.

The prediction of ASM species in a solution was evaluated by creating Pourbaix diagrams. Fig. 8A shows the Pourbaix diagram for an As concentration of 0.5 mM and S concentration of 0.25 mM (the maximum concentration of $H_2S$ at equilibrium in the pH 7.2 experiment). At the studied pH and $E_h$ range ($E_h$ = −200±50 mV, measured), $As_2S_3$ and AsS are the minerals expected to precipitate for pH values close to 6 within the range of $E_h$ in the treatments. With increasing pH, the formation of AsS is limited to more reducing conditions, and $As_2S_3$ is the more likely precipitate up to a pH of 7.0, thereafter, thioarsenites species become predominant, limiting the precipitation of ASM. The thermodynamic stability areas for $As_2S_3$ and AsS predicted in this study are similar to the Pourbaix diagrams constructed by Lu and Zhu (2011) for a system containing 1 mM of S and As. Fig. 8B was built to show the formation of thioarsenites as a function of the pH and $H_2S$ concentration. As the concentration of $H_2S$ increases, the minimum pH at which thioarsenites could be formed decreases. The same trend was predicted by Wilkin (2003) when studying the solubility of As in the presence of S. In conclusion, for the experimental $E_h$ range, the formation of $As_2S_3$ and AsS is expected over the mildly acidic range of pH; at circumneutral and higher pH values, the formation of thioarsenite species becomes dominant and limits the precipitation of ASM, however, for any precipitation that does occur it would be predominantly in the form of $As_2S_3$.

### 4.3. As toxicity effect on the methanogenic activity

Soluble As was highly toxic to the methanogenic archaea community. The soluble $As^{III}$ formed from the reduction of $As^V$ caused a severe inhibition in the methanogenic activity, as demonstrated by the accumulation of acetate and the extremely low $CH_4$ production. However, the inhibition was largely attenuated by the removal of As throughout the precipitation of ASM. The high toxicity of $As^{III}$ in methanogenic consortium has been established by Sierra-Alvarez (2004). Very low $As^{III}$ concentrations are enough to greatly

inhibit the methanogenic activity, the 80% inhibitory concentrations were 23.5 μM and 79.2 μM, for the acetoclastic and hydrogenotrophic methanogenesis, respectively. The $As^{III}$ concentration in this study was 500 μM. The high concentration of $As^{III}$ (produced by the bioreduction of $As^{V}$) greatly inhibited the metabolic activity of the methanogenic community.

### 4.5. Conclusions

- This study demonstrates that the biological reduction of $As^{V}$ and $SO_4^{2-}$ by a mixed microbial culture in a methanogenic biofilm can be harnessed to precipitate ASM.
- The extent and rate of As removal is highly influenced by the pH, with the highest rates achieved at mildly acidic conditions.
- The pH would also impact the mineralogical composition of the ASM, with an increase in orpiment compared to realgar at neutral pH.
- Arsenic biomineralization can potentially be used to promote the immobilization of As groundwaters by stimulating the $As^{V}$ and $SO_4^{2-}$ reducing bacteria.

## Supplementary Material

Refer to Web version on PubMed Central for supplementary material.

## Acknowledgments

The work presented here was funded by a grant of the National Institute of Environment and Health Sciences-supported Superfund Research Program (NIH ES-04940). Portions of this research were carried out at Stanford Synchrotron Radiation Laboratory, a National User Facility operated by Stanford University on behalf of the U.S. Department of Energy, Office of Basic Energy Sciences. We are also grateful to the University Spectroscopy and Imaging Facility at the University of Arizona for the SEM-EDS analysis. This work was partially funded by a Water Sustainability Program Fellowship, The University of Arizona, awarded to Lucia Rodriguez-Freire.

## 6. References

APHA. Standard methods for the examination of water and wastewater. APHA, AWWA and WEF; Washington D.C: 1999.

Battaglia-Brunet F, Crouzet C, Burnol A, Coulon S, Morin D, Joulian C. Precipitation of arsenic sulphide from acidic water in a fixed-film bioreactor. Water Research. 2012; 46(12):3923–3933. [PubMed: 22608606]

Demergasso CS, Chong G, Escudero L, Mur JJP, Pedros-Alio C. Microbial precipitation of arsenic sulfides in Andean salt flats. Geomicrobiology Journal. 2007; 24(2):111–123.

Elferink SJWH, Visser A, Pol LWH, Stams AJM. Sulfate reduction in methanogenic bioreactors. Fems Microbiology Reviews. 1994; 15(2–3):119–136.

Hoeft SE, Kulp TR, Stolz JF, Hollibaugh JT, Oremland RS. Dissimilatory arsenate reduction with sulfide as electron donor: Experiments with Mono Lake Water and isolation of strain MLMS-1, a chemoautotrophic arsenate respirer. Applied and Environmental Microbiology. 2004; 70(5):2741–2747. [PubMed: 15128527]

Huber R, Sacher M, Vollmann A, Huber H, Rose D. Respiration of arsenate and selenate by hyperthermophilic archaea. Systematic and Applied Microbiology. 2000; 23(3):305–314. [PubMed: 11108007]

Jonsson J, Sherman DM. Sorption of As(III) and As(V) to siderite, green rust (fougerite) and magnetite: Implications for arsenic release in anoxic groundwaters. Chemical Geology. 2008; 255(1–2):173–181.

Kirk MF, Roden EE, Crossey LJ, Brearley AJ, Spilde MN. Experimental analysis of arsenic precipitation during microbial sulfate and iron reduction in model aquifer sediment reactors. Geochimica Et Cosmochimica Acta. 2010; 74(9):2538–2555.

Ledbetter RN, Connon SA, Neal AL, Dohnalkova A, Magnuson TS. Biogenic mineral production by a novel arsenic-metabolizing thermophilic bacterium from the Alvord Basin, oregon. Applied and Environmental Microbiology. 2007; 73(18):5928–5936. [PubMed: 17630300]

Lee JH, Kim MG, Yoo BY, Myung NV, Maeng JS, Lee T, Dohnalkova AC, Fredrickson JK, Sadowsky MJ, Hur HG. Biogenic formation of photoactive arsenic-sulfide nanotubes by *Shewanella* sp strain HN-41. Proceedings of the National Academy of Sciences of the United States of America. 2007; 104(51):20410–20415. [PubMed: 18077394]

Liu B, Wu WF, Zhao YJ, Gu XY, Li S, Zhang XX, Wang Q, Li RH, Yang SG. Effects of ethanol/$SO_4^{2-}$ ratio and pH on mesophilic sulfate reduction in UASB reactors. African Journal of Microbiology Research. 2010; 4(21):2215–2222.

Lu P, Zhu C. Arsenic Eh-pH diagrams at 25 degrees C and 1 bar. Environmental Earth Sciences. 2011; 62(8):1673–1683.

Macy JM, Santini JM, Pauling BV, O'Neill AH, Sly LI. Two new arsenate/sulfate-reducing bacteria: mechanisms of arsenate reduction. Archives of Microbiology. 2000; 173(1):49–57. [PubMed: 10648104]

Murcott, S. An international sourcebook 2012. IWA Publishing; London: 2012. Arsenic contamination in the World.

Newman DK, Beveridge TJ, Morel FMM. Precipitation of arsenic trisulfide by *Desulfotomaculum auripigmentum.* Applied and Environmental Microbiology. 1997; 63(5):2022–2028. [PubMed: 16535611]

O'Day PA, Vlassopoulos D, Root R, Rivera N. The influence of sulfur and iron on dissolved arsenic concentrations in the shallow subsurface under changing redox conditions. Proceedings of the National Academy of Sciences of the United States of America. 2004; 101(38):13703–13708. [PubMed: 15356340]

Onstott TC, Chan E, Polizzotto ML, Lanzon J, DeFlaun MF. Precipitation of arsenic under sulfate reducing conditions and subsequent leaching under aerobic conditions. Applied Geochemistry. 2011; 26(3):269–285.

Rittle KA, Drever JI, Colberg PJS. Precipitation of arsenic during bacterial sulfate reduction. Geomicrobiology Journal. 1995; 13(1):1–11.

Saunders JA, Lee MK, Shamsudduha M, Dhakal P, Uddin A, Chowdury MT, Ahmed KM. Geochemistry and mineralogy of arsenic in (natural) anaerobic groundwaters. Applied Geochemistry. 2008; 23(11):3205–3214.

Sierra-Alvarez R, Cortinas I, Yenal U, Field JA. Methanogenic inhibition by arsenic compounds. Applied and Environmental Microbiology. 2004; 70(9):5688–5691. [PubMed: 15345461]

Sierra-Alvarez R, Field JA, Cortinas I, Feijoo G, Teresa Moreira M, Kopplin M, Jay Gandolfi A. Anaerobic microbial mobilization and biotransformation of arsenate adsorbed onto activated alumina. Water Research. 2005; 39(1):199–209. [PubMed: 15607178]

Tang K, Baskaran V, Nemati M. Bacteria of the sulphur cycle: An overview of microbiology, biokinetics and their role in petroleum and mining industries. Biochemical Engineering Journal. 2009; 44(1):73–94.

Tapia-Rodriguez A, Luna-Velasco A, Field JA, Sierra-Alvarez R. Anaerobic bioremediation of hexavalent uranium in groundwater by reductive precipitation with methanogenic granular sludge. Water Research. 2010; 44(7):2153–2162. [PubMed: 20060558]

Truper HG. Sulphur metabolism in *Thiorhodaceae* .II. stoichiometric relationship of $CO_2$ fixation to oxidation of hydrogen sulphide and intracellular sulphur in *Chromatium Okenii*. Antonie Van Leeuwenhoek Journal of Microbiology and Serology. 1964; 30(4):385. &.

US-EPA. National primary drinking water regulations; arsenic and clarifications to compliance and new source contaminants monitoring. 2001.

van Lis R, Nitschke W, Duval S, Schoepp-Cothenet B. Arsenics as bioenergetic substrates. Biochimica Et Biophysica Acta-Bioenergetics. 2013; 1827(2):176–188.

Welch AH, Westjohn DB, Helsel DR, Wanty RB. Arsenic in ground water of the United States: Occurrence and geochemistry. Ground Water. 2000; 38(4):589–604.

Wilkin RT, Wallschlager D, Ford RG. Speciation of arsenic in sulfidic waters. Geochemical Transactions. 2003; 4:1–7.

## Highlights

- The biological reduction of $As^{V}$ and $SO_4^{2-}$ resulted in arsenic sulfide precipitation.
- Arsenic sulfides formed were a mixture of $As_2S_3$ and AsS.
- The bioprecipitation of arsenic sulfides is enhanced at mildly-acidic pH.
- A higher proportion of $As_2S_3$ over AsS is obtained at circumneutral pH.
- The methanogenic inhibition by As is reversed by arsenic sulfide mineral formation.

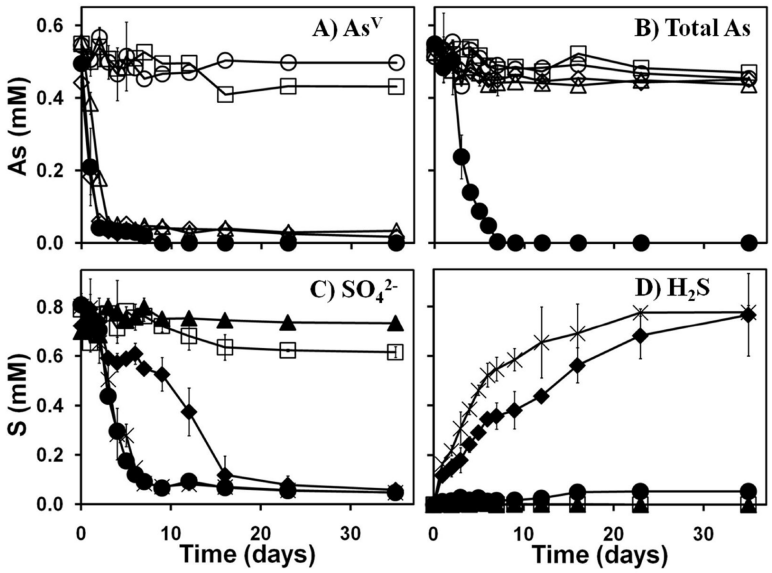


**Fig. 1.**

Precipitation of ASM through the biological mediated reduction of 0.5 mM of $As^V$ and 0.75 mM of $SO_4^{2-}$ using 14 mM of ethanol as the electron donor at pH 6.1. Dissolved $As^V$ concentration of (A); total As concentration (B); $SO_4^{2-}$ concentration (C); and total $H_2S$ as the sum of $H_2S(g)$ and all the aqueous species (mmol/$L_{liq}$ or mM) (D). The complete treatment containing inoculum, $As^V$, $SO_4^{2-}$ and ethanol (●); Inoculum ,$SO_4^{2-}$ and ethanol (x), Inoculum $As^V$ and ethanol (◇),inoculum and $SO_4^{2-}$ (◆), inoculum and $As^V$ (Δ), inoculum and ethanol (+); Sterile controls with $As^V$ and ethanol (◯), the sterile control with $SO_4^{2-}$ and ethanol (▲) and the combined reduction sterile control with $SO_4^{2-}$ and $As^V$ with ethanol (□). Treatments with value zero over the time course of the experiment are not shown: treatments lacking As in panels A and B, and treatments lacking S in panels C and D.

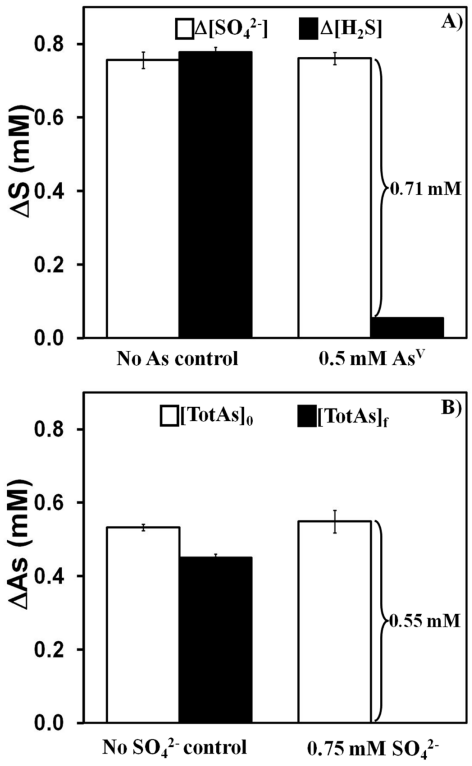


**Fig. 2.**

S and As concentration loss between day 0 and the end of the experiment (day 35) for the treatment at pH 6.1. Panel (A) show the S loss for the inoculated control with no $As^V$ addition and for the complete treatment; the difference in $SO_4^{2-}$ is represented in the open column and the formation of $H_2S$ in the filled column. Panel (B) illustrates the total As loss in the inoculated control lacking $SO_4^{2-}$ and in the complete treatment; initial total As concentration is represented with the open column and the final total As concentration with the filled column.

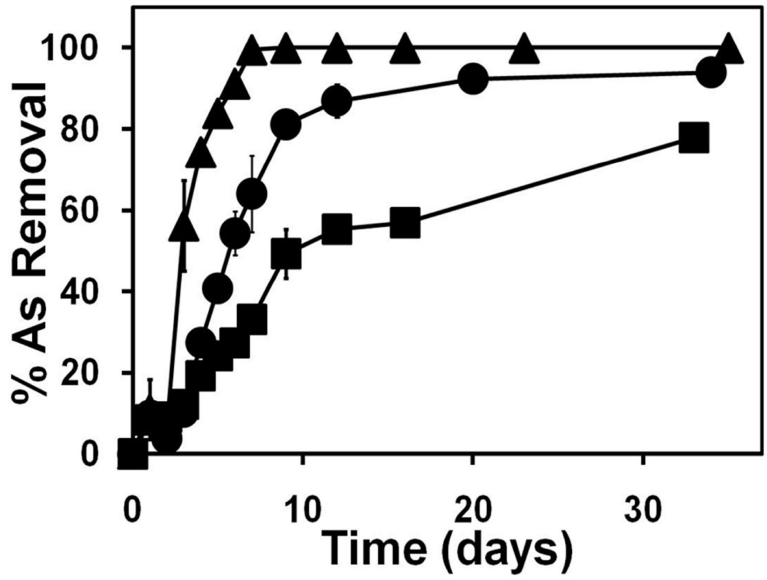


**Fig. 3.**

Total As removal over the course of the experiments shown as the As removal percentage at the three investigated pH 6.1 (▲), 6.5 (●) and 7.2 (■).

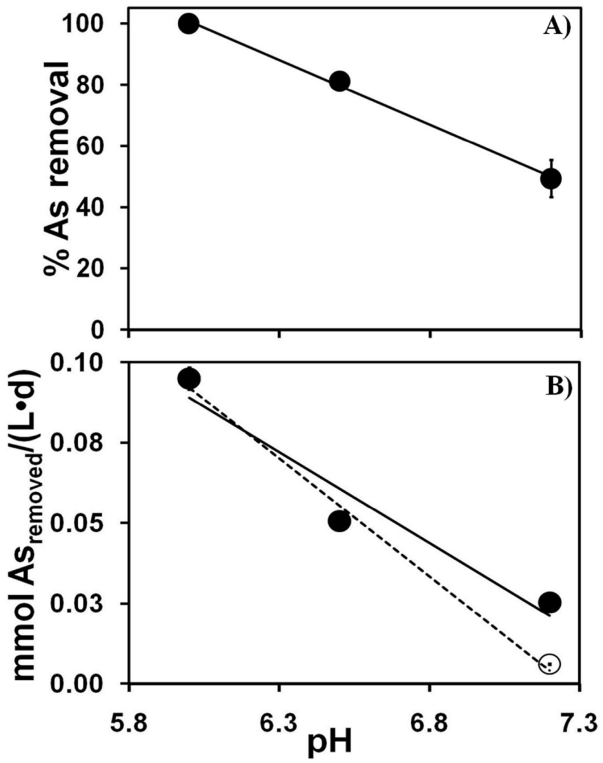


**Fig. 4.**

Relationship between the total As removal and the pH. Panel (A) illustrates the trend and linear regression line for As removal as a function of the pH at day 9. The linear regression equation was obtained and the relationship between the As removal and pH can be represented by the linear equation %Asremoval = A – B•pH. The constants and the R-squared are: A = 355.3 %As, B = 42.4 %As, $R^2$ = 0.9973. Panel (B) shows the total As removal rate (mmolAs/(L•d)) as a function of the pH. The total As removal rate was calculated using the slope for the first 6 d at pH 6.1, and for the first 9 d at pH 6.5. At pH 7.2, two different As removal rates were observed, high rate, from day 0 to 9 (●), and a lower rate, from day 9 until the end of the experiment (◯). The rate of As removal is related to the pH by linear regression equations considering the higher rate at pH 7.2 (continuous line) and the lower rate at pH 7.2 (dashed line). The constants and the R-squared are: higher rate at pH 7.2, A = 0.4286 mmolAs/(L•d), B = 0.0566 mmolAs/(L•d), and $R^2$ = 0.9374; lower rate at pH 7.2, A = 0.5324 mmolAs/(L•d), B = 0.0734 mmolAs/(L•d), and $R^2$ = 0.9911.

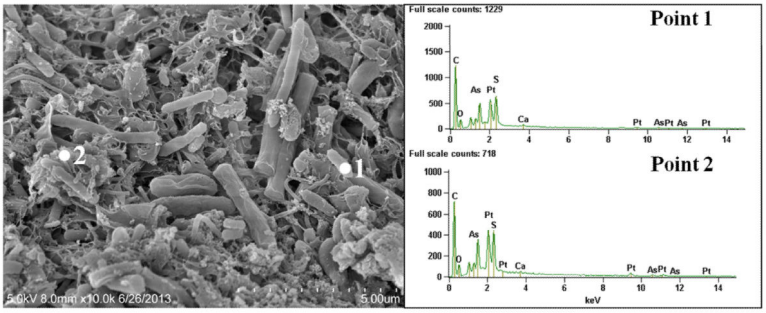


**Fig. 5.**

SEM-EDS analysis of the precipitate from the complete treatment at pH 6.1 containing 0.5 mM $As^{V}$, 0.75 mM $SO_4^{2-}$ and 14 mM ethanol after 21 days of incubation.

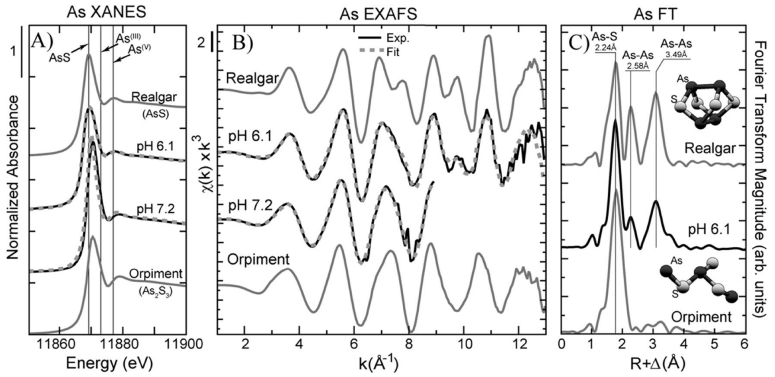


**Fig. 6.**

Arsenic K-α x-ray absorption spectra of the solids precipitated in the experiments at pH 6.1 and 7.2. Panel A shows the XANES spectra (solid lines) for As-S mineral fit (stippled lines) by least squares linear combination to standards (gray lines) of realgar (AsS) and orpiment ($As_2S_3$), vertical lines indicate the diagnostic As species position (± 1 eV): 11869 = arsenic sulfide; 11872 = $As^{III}$; 11875 = $As^{V}$. Panel B shows the EXAFS spectra for the experimental data (black lines) and least squares linear combination fits (stippled lines) to As-S minerals. Fits and reported error are given in Table S1. The Fourier Transform (FT) of the references and the pH 6.1 sample are shown in Panel C; vertical bars indicate As-backscatter distances. The FT is not shown for pH 7.2 because EXAFS were cut at k($Å^{-1}$) = 9 and did not allow comparison to pH = 6.1.

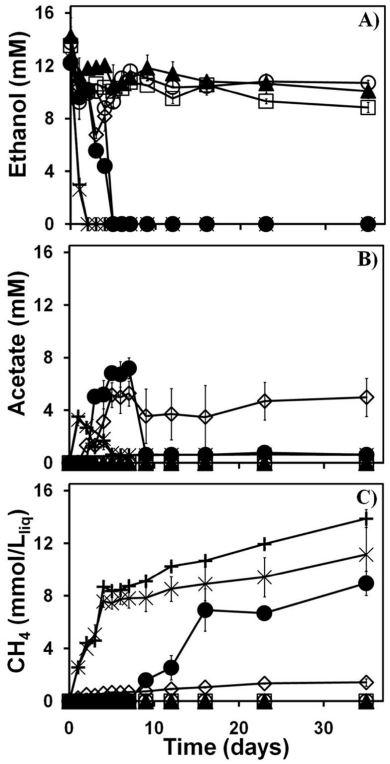


**Fig. 7.**

Conversion of ethanol 14 mM in the experiment conducted at pH 6.1. Panels show the ethanol concentration (A); acetate concentration (B); and, $CH_4$ production (C). The complete treatment containing inoculum, $As^V$, $SO_4^{2-}$ and ethanol (●); Inoculum ,$SO_4^{2-}$ and ethanol (x), Inoculum $As^V$ and ethanol (◇), inoculum and $SO_4^{2-}$ (◆), inoculum and $As^V$ (Δ), inoculum and ethanol (+); Sterile controls with $As^V$ and ethanol (◯), the sterile control with $SO_4^{2-}$ and ethanol (▲) and the sterile control with $SO_4^{2-}$, $As^V$ and ethanol (□). Treatments lacking ethanol addition (with zero values over the time course of the experiment) are not shown.

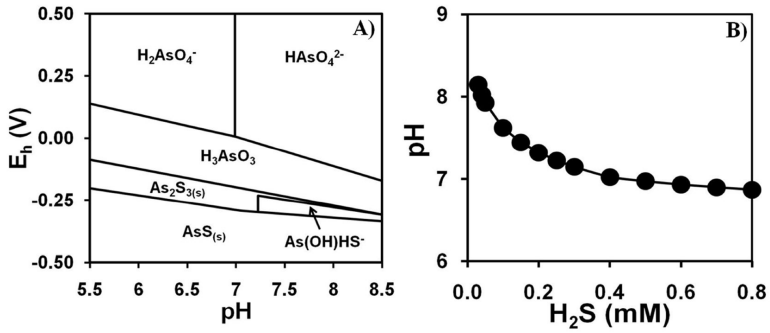


**Fig. 8.**

Predicted stable mineral and aqueous phases at equilibrium, including thioarsenite species. Panel A: Pourbaix diagram for As minerals at 25°C and 1 atm showing the stability fields for solid phases at the conditions the orpiment and realgar, in a solution with 0.5 mM of As and 0.25 mM of S. Panel B: Minimum pH enabling formation of thioarsenite species as a function of the $H_2S$ equilibrium concentration, ranging from 0 to 0.75 mM (maximum $H_2S$ production due to $SO_4^{2-}$ reduction)

**Table 1**

Table 1 Summary of the important reaction to consider in the microcosm studies

| | |
|---|---|
| **Ethanol acetogenesis:** | |
| $CH_3CH_2OH + H_2O \rightarrow CH_3COO^- + 2H_2 + H^+$ | **Eq. 1** |
| **Acetoclastic methanogenesis:** | |
| $CH_3COO^- + H^+ \rightarrow CH_4 + CO_2$ | **Eq. 2** |
| **Hydrogenotrophic methanogenesis:** | |
| $4\ H_2 + CO_2 \rightarrow CH_4 + 2\ H_2O$ | **Eq. 3** |
| **Sulfate reduction coupled to $H_2$ oxidation:** | |
| $SO_4^{2-} + 4\ H_2 + 2\ H^+ \rightarrow H_2S + 4\ H_2O$ | **Eq. 4** |
| **Arsenate reduction coupled to $H_2$ oxidation:** | |
| $H_2AsO_4^- + H_2 + H^+ \rightarrow H_3AsO_3 + 2\ H_2O$ | **Eq. 5** |
| **Mineralization:** | |
| $xH_3AsO_3 + yHS^- + (3x\text{-}y)\ H^+ \rightarrow As_xS_{y(s)} + 3xH_2O$ | **Eq. 6** |
| x = y = 1, realgar (α-AsS) formation | |
| x = 2; y = 3, orpiment ($As_2S_3$) formation | |

**Table 2**

Experimental results at different times for the precipitation of As-S mineral treatments at different pH (6.1, 6.45 and 7.1)

| Experiment | $t_{exp}$ (d) | $pH_t$ | $[TotAs]_t$ (mM) | $[SO_4^{2-}]_t$ (mM) | $[H_2S]_t$ (mM) | $S_{loss}/AS_{loss}$ ‡ |
|---|---|---|---|---|---|---|
| pH = 6.1 | 0 | 6.17 | 0.55±0.01 | 0.81±0.03 | 0.00±0.00 | -- |
| | 6 | 5.93 | 0.05±0.02 | 0.12±0.01 | 0.01±0.00 | 1.34 |
| | 9 | 5.97 | 0.00±0.00 | 0.07±0.01 | 0.02±0.01 | 1.32 |
| | 12 | 5.90 | 0.00±0.00 | 0.09±0.01 | 0.03±0.01 | 1.25 |
| | 35 | 5.96 | 0.00±0.00 | 0.05±0.00 | 0.05±0.00 | 1.29 |
| pH = 6.45 | 0 | 6.44 | 0.51±0.00 | 0.78±0.02 | 0.00±0.00 | -- |
| | 6 | 6.49 | 0.25±0.03 | 0.35±0.02 | 0.05±0.01 | 1.47 |
| | 9 | 6.49 | 0.10±0.00 | 0.20±0.02 | 0.04±0.01 | 1.31 |
| | 12 | 6.47 | 0.07±0.02 | 0.17±0.04 | 0.04±0.01 | 1.31 |
| | 34 | 6.49 | 0.03±0.00 | 0.14±0.01 | 0.03±0.00 | 1.27 |
| pH = 7.1 | 0 | 7.13 | 0.51±0.01 | 1.09±0.05 | 0.00±0.00 | -- |
| | 6 | 7.15 | 0.39±0.01 | 0.87±0.05 | 0.08±0.01 | 1.27 |
| | 9 | 7.15 | 0.27±0.03 | 0.57±0.01 | 0.11±0.00 | 1.80 |
| | 12 | 7.19 | 0.24±0.00 | 0.38±0.03 | 0.26±0.02 | 1.72 |
| | 33 | 7.15 | 0.12±0.00 | 0.38±0.00 | 0.25±0.04 | 1.19 |

‡S and As losses are defined as the difference between the total initial concentration and the concentration at time t:

$S_{loss} = (SO_4^{2-} + H_2S)_0 - (SO_4^{2-} + H_2S)_t$

$As_{loss} = (TotAs)_0 - (TotAs)_t$